ELSEVIER ELSEVIER

Contents lists available at ScienceDirect

Extreme Mechanics Letters

journal homepage: www.elsevier.com/locate/eml



Temperature dependence of contact quality inducing suppression of stick-slip friction



Liming Zhao, Penghui Cao*

Department of Mechanical and Aerospace Engineering, University of California, Irvine, CA 92697, USA Department of Materials Science and Engineering, University of California, Irvine, CA 92697, USA

ARTICLE INFO

Article history: Received 19 January 2021 Received in revised form 24 February 2021 Accepted 4 March 2021 Available online 10 March 2021

Keywords: Stick-slip Friction Graphene Contact quality

ABSTRACT

Atomic-scale stick-slip friction of monolayer graphene on a copper substrate is computationally studied at a wide range of temperatures, which reveals strong temperature dependence of friction force and friction mode. The increase in temperature distorts regular stick-slip behavior and causes a nonlinear decrease of friction force, demonstrating a friction behavior transition from athermal friction to thermally activated. By analyzing atomic morphologies, the true contact area, defining the number of atoms interacting across the interface, shows a weak temperature dependence, yet the quality of interfacial contact substantially varies with temperature. Spatial distributions of atomic friction force uncover the significant effect of Moiré superlattices, that act as strong pinning sites at low temperatures, partly change to pushing due to nonconcurrent atomic jumps at high temperatures, which leads to a chaotic friction mode with reduced lateral force. Additionally, we demonstrate the role of superlattices in strengthening friction and dictating the periodic stick-slip motion of interfacial sliding.

© 2021 Elsevier Ltd. All rights reserved.

Atomic-scale stick-slip friction involving fundamental friction mechanisms is an intriguing phenomenon, in which two contacting surfaces slide over each other in a regular stick and slip manner [1,2]. Prandtl [3] and Tomlinson [4] nearly a century ago proposed a reduced-ordered PT model interpreting this complex friction behavior. The simple model considers a tip attached via a spring moving in a potential energy landscape formed by the interfacial atomic interaction. The tip that initially sticks in a deep local energy minimum glides to the neighboring local minimum with a critical lateral force, at which the energy barrier is vanished and slip motion occurs. If one of the contacting surfaces is crystalline, the potential energy landscape is therefore periodic and the stick-slip motion repeats, appearing as regular stickslip friction. Based on this mechanistic picture, approaches to agitating the tip out of sticking potential energy minimum have been proposed to tune the frictional response. For example, by applying small-amplitude normal vibration, the friction force can be considerably lowered, erasing stick-slip motion manifested as a transition from regular sawtooth friction to smooth sliding [5,6].

Apart from mechanical excitation, thermal vibration that regulates the hopping rate from a present local energy minimum into an adjacent one, governs the nonlinear dependence of friction on temperature [7–11]. With increasing temperature, for instance,

E-mail address: caoph@uci.edu (P. Cao).

friction force decreases exponentially [10], and in some situations the friction resistance can be nearly vanished due to the prominent role of thermal effects, leading to thermolubricity [8]. While the theoretical model phenomenologically interprets the experimental observations, the atomic-scale friction mechanisms underlying temperature dependence of frictional behaviors such as friction force reduction and stick-slip distortion remain as fundamental questions.

We report a computational study of interfacial friction in graphene island supported on Cu (111) surface, a system that has been extensively studied because Cu (111) is mainly adopted as the substrate for chemical vapor deposition of graphene [12, 13]. On the other hand, graphene, acting as the thinnest solid lubricant, is considered an excellent candidate for reducing friction [14]. Originating from lattice mismatch in graphene and Cu (111) substrate, Moiré patterns appear in the interface [12], which presumably influences the interfacial sliding behavior. Therefore, the main motivation of this study is to investigate the frictional response of graphene-Cu over a wide range of temperatures and to understand the role of Moiré patterns in governing stickslip friction. By performing atomistic simulations of friction at a variety of temperatures, we find that increasing temperature results in the distortion of the regular stick-slip friction, in the form of reduced frictional force, suppressed stick-slip mode, and shifted stick-slip periodicity. We find the true contact area, which represents the number of atoms interacting across the interface, exhibits weak temperature sensitivity. Yet, the interfacial atomic

^{*} Corresponding author at: Department of Mechanical and Aerospace Engineering, University of California, Irvine, CA, USA.

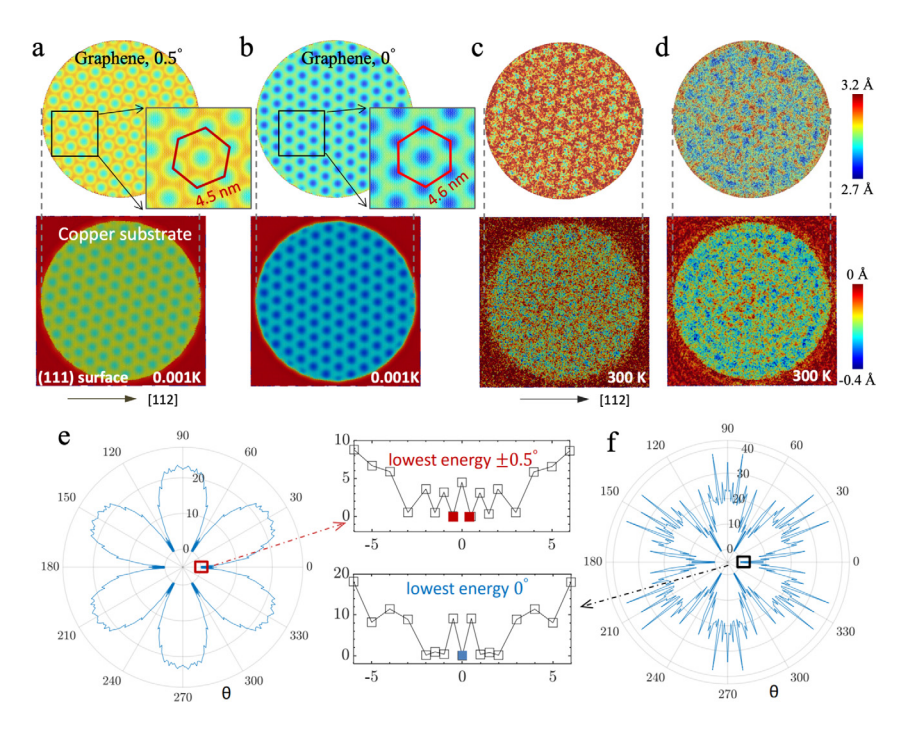


Fig. 1. (a) Surface morphologies of graphene and the copper substrate at 0.001 K. Graphene armchair and copper [112] direction have a misorientation angle $\theta = 0.5^{\circ}$. (b) The morphologies in the presence of normal stress. Armchair direction and copper [112] are aligned. (c-d) The same morphology analysis for the temperature of 300 K. (e-f) Free energy variations with rotation angle θ show multiple metastable states, indicated by local energy minimum. For free-standing graphene (e), the lowest energy state locates at 0.5°. (f) In the presence of normal load, the potential energy landscape is roughed, with the lowest energy being changed to 0°.

forces, defining the contacting quality, reveal Moiré superlattices act as the primary pinning sites at cryogenic temperatures and partially transform to pushing sites at high temperatures, causing the suppression of stick-slip friction.

The friction system consists of a monolayer graphene supported on Cu (111) surface. The interaction between Cu atoms is described by an embedded atom model (EAM) potential [15], and the covalent bonds of C–C in graphene are modeled by the adaptive intermolecular reactive empirical bond order (AIREBO) force field [16]. The Lennard-Jones potential, developed to capture the interlayer distance and adhesion strength [17], is used to simulate the interactions between Cu substrate and graphene. The graphene flake with a diameter of 50 nm is first created and put on the Cu slab, which has a lateral dimension of 53 nm × 53 nm and a thickness of 2.5 nm. We first relax the system at constant temperature condition for 200 ps, using Nose–Hover [18,19] thermostat to control temperature.

We connect the graphene to a rigid stage through a lateral spring, and the stage is moving at a constant velocity, which enables interfacial sliding friction [20]. We test different elastic constants of spring, including 5, 50, 500, and 5,000 eV/Å², and find that the value, controlling how fast friction reaches a steadystate, does not qualitatively influence the friction behavior. The results reported here are from the spring constant of 50 eV/Å², except the extremely-low temperature 0.001 K, at which 5,000 $eV/Å^2$ is used for the sake of computational efficiency due to large frictional force. To model a normal load from the rigid stage, we apply a uniform force 0.04 nN/atom to all the graphene atoms, and we further relax the whole system for another 100 ps in at a constant temperature. During friction motion, the stage is moving at the velocity 10 nm/ns, and the frictional force is measured by the lateral spring force $F = k(x_s - x_g)$, where kis the spring constant, x_s is stage position, and x_g represents the location of center of mass of the graphene. We characterize the contact quality in graphene and copper by measuring the atomic forces. To minimize the random thermal fluctuation effect on the interfacial forces, we perform energy minimization and relax the system to the nearest local energy minimum. Therefore, the atomic forces are analyzed on quasistatic states, and this analysis qualitatively characterizes the interfacial contact nature [21].

Fig. 1a-b shows how the graphene and copper surface morphologies vary with applying normal force at a low temperature of 0.001 K. In the absence of normal load (Fig. 1a), the graphene flake reveals clear Moiré pattern superlattice. The lattice periodicity of 4.5 nm is consistent with the experimental measurements [13]. In the relaxed system, the graphene indicates a subtle rotation angle θ = 0.5°, defined as the relative orientation between graphene armchair and Cu [112] directions. It is noted that the superlattice pattern is dictated by graphene and copper lattice constants, as well as this relative orientation θ (see section 1 in supplementary information). With the normal force applied to graphene, the relaxed system displays a 0 angle (Fig. 1b), implying the graphene under the normal load has reversely rotated 0.5°. To understand the thermodynamic driving force underlying graphene rotation, we calculate the potential energy landscape of graphene with respect to the angle θ , as shown in Fig. 1ef. The energy profile appears a periodicity of 60° due to the hexagonal symmetry of graphene, where the lowest free energy state occurs at $\pm 0.5^{\circ}$ for the graphene without applied load (see Fig. 1e). In the presence of the normal force (Fig. 1f), the free energy variation with angle has been altered and roughed, and the energetically favorable state transforms to 0°. This subtle graphene rotation is related to the apparent transformation of the superlattice. While the graphene morphology reveals clear Moiré superlattices at low temperatures, those patterns are vanishing as increasing temperature, such as 300 K (Fig. 1c-d), as a result of thermal roughening [22].

With the understanding of the system morphologies and energy states, we select the lowest energy configuration for friction simulations. Fig. 2a shows friction force as a function of sliding distance at three different temperatures, as indicated. In the steady-state friction regime, the force-displacement curves show stick-slip behavior, reflected by the serrated motion. When changing temperature from 0.001 through 0.01 to 300 K, there

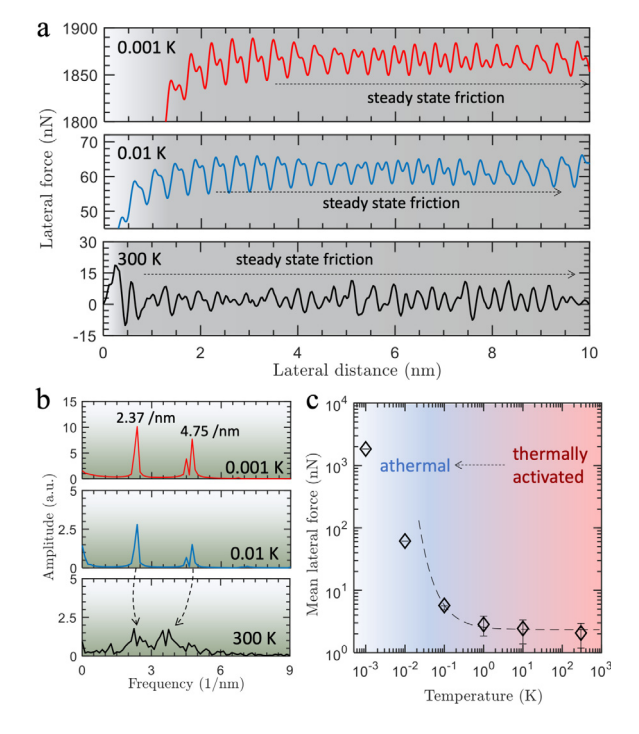


Fig. 2. (a) Friction force as a function of sliding distance showing stickslip motion in the steady sliding state (kinetic friction). The red, blue, and black curves denote system temperatures of 0.001 K, 0.01 K, and 300 K, respectively. (b) The corresponding Fourier transformations of the force traces in (a). The regular stick–slip friction transforms into a chaotic stick–slip regime with increasing temperature. (c) Temperature dependence of average lateral friction forces. The dashed line is the best fitted Arrhenius-like formula. (For interpretation of the references to color in this figure legend, the reader is referred to the web version of this article.)

are two notable trends that can be discerned. The regular and periodic stick–slip motion, occurring at low temperatures, becomes irregular or chaotic at high temperatures. To quantify the temperature-induced regularity, Fig. 2b demonstrates the corresponding spectrums of Fourier transformation, exhibiting two distinct peaks at 2.37/nm and 4.75/nm at 0.001 K. The primary peak (left) with a large periodicity of 0.42 nm corresponds to the lattice periodicity of graphene along the armchair direction. The secondary peak with a periodicity of 0.21 nm is related to graphene atoms jumping between the potential vacancy sites on the Cu (111) surface (see Figure S3–4 in SI). One can see as the temperature rises, the two stick–slip modes become weak, and at 300 K, the periodic friction motions are shifted and weakened, suggesting the role of temperature in distorting the regularity of stick–slip motion.

Besides the observed periodic to chaotic stick-slip transformation, temperature rise considerably induces the reduction of friction force and the stick-slip amplitude (Fig. 2a, c). According to activation theory [23], the hopping frequency from the current potential energy minimum to a neighboring one becomes more likely at a higher temperature, and therefore a lower lateral force is necessary to maintain the sliding. In two-dimensional material friction, for example, the force is observed to increase exponentially with decreasing temperature [10]. Fig. 2c, plotting lateral force against temperature, exhibits this exponential dependency of friction on temperature up to a point, 0.1 K. Further lowering the temperature leads to a deviation from this exponential scaling relationship. This transition on frictional force suggests the thermally activated friction, predominating the high-temperature regime, changes to athermal-like sliding at low temperatures. It is worth noting that the friction transition is induced by varying

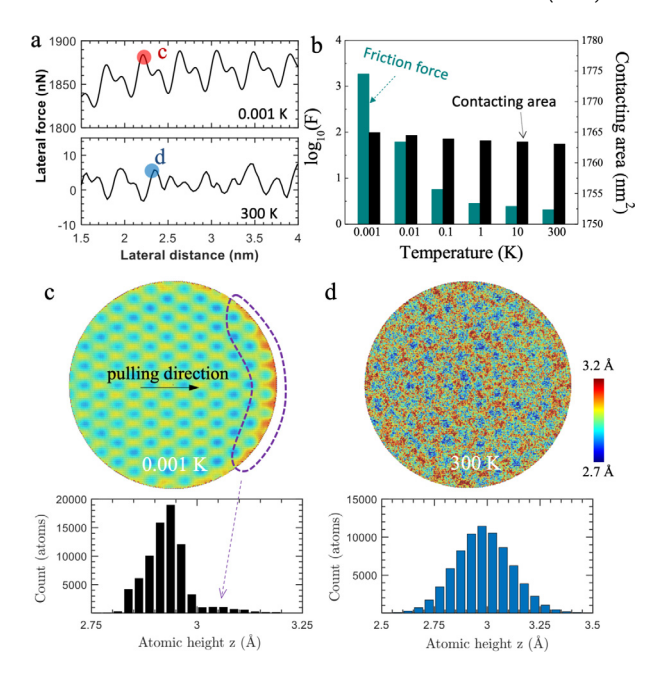


Fig. 3. (a) Enlarged view of the friction force traces at temperatures of 0.001 K and 300 K showing the peak friction states (marked by c and d) before slip motion. (c-d) The corresponding graphene morphologies in the peak friction indicated in (a). (b) Variations of averaged friction force and true contact area with temperature.

temperatures at a fixed high stage velocity of 10 nm/ns. When lowering the speed, it is expected that the crossover can occur at a reduced temperature [7]. Because of the timescale limitation inherent in the molecular dynamics, alternative approaches such as potential energy landscape modeling [24], which has been used to study slow strain rate deformation of solids [25–27], should enable studies of interfacial friction at low velocity.

To find the root cause behind the temperature-dependent friction, we carefully examine the interfacial contacting nature underlying friction motion. Fig. 3c-d shows the graphene morphologies, corresponding to the peak friction state as labeled in Fig. 3a, at temperatures 0.001 K and 300 K, respectively. The superlattice patterns in low-temperature friction are essentially retained. It is interesting to note the leading friction front of graphene is tilted up with relatively high height, which reflects a nonuniform response of the atomic thin-film subjected to a directional pulling. This lifted front edge also demonstrates how the graphene adapts itself in accommodating the friction resistance. In contrast, the Gaussian-like distribution of graphene height at 300 K (Fig. 3d), manifesting the balanced out-of-plane roughness, is considered to be predominantly controlled by thermal fluctuation. In nanoscopic friction theory [28], the friction force is argued to increase linearly with the contact area. To reveal the contribution of the interfacial contact area, we determine the true contact area, defining the number of atoms chemically interacting across the interface. By computing how many graphene atoms are in intimate contact with the substrate within a cutoff distance 4 Å, the black bars in Fig. 3b show variation of the true contact area with system temperature. The contact area slightly increases with decreasing the temperature, but it alone is inadequate to explain the large increase of friction force. It motivates us to look into the contacting quality, represented by the atomic friction force, between graphene and the substrate.

Before measuring the interfacial atomic force, we first perform energy minimization to bring the system to its inherent local energy minimum state, eliminating the random thermal fluctuation effect. It is noted, while this energy minimization could alter

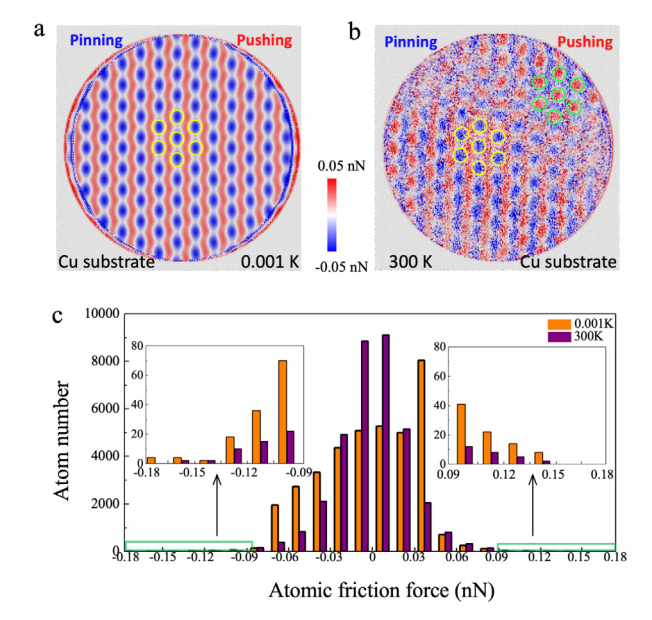


Fig. 4. (a–b) Spatial distribution of atomic friction forces on the substrate surface at 0.001 K and 300 K, respectively. The blue color with a negative magnitude of force indicates local pinning sites, hindering/dragging graphene movement. The red-colored regions with positive force, promoting graphene forward motion, are local pushing sites. (c) Histogram of atomic forces shown in (a) and (b). (For interpretation of the references to color in this figure legend, the reader is referred to the web version of this article.)

the force magnitude, it does not change the frictional behavior qualitatively [21]. The interfacial atomic force, exerted by the ith copper atom on graphene, is calculated as $f_i = f_i(x_p)$ – $f_i(x_0)$, where x_p is the peak friction state, and x_0 is the initial local minimum state. Fig. 4a shows the spatial distribution of the atomic force on the top layer of copper. The negative forces (blue color), pointing to the negative direction, are against the motion, known as pinning forces. The red-colored regions with positive forces are pushing sites, which help the forward motion of graphene. The arrangement of pinning sites at low temperatures (Fig. 4a) displays a hexagonal pattern, which is attributed to the Moiré superlattice interaction(see discussion of Fig. 5). At the temperature of 300 K, even though the hexagonal force patterns can barely be seen, they become blurred and twisted, implying effects of thermal. More interestingly, some of the pinning sites change to pushing points (green circle in Fig. 4b), which would lower the total friction force. The coexistence of pinning-pushing sites and the dislocation-like boundary separating the sites are evidence of nonconcurrent stick-slip motion. This nonuniform motion can be attributed to heterogeneous energy barrier crossing and early jumping of the partial graphene atoms into the neighboring local minimum. In Fig. 4c, we plot the corresponding histogram distribution of atomic force at 0.001 K and 300 K. Both of the distributions, exhibiting a majority of low magnitude atomic forces, are skewed negatively, which gives rise to a negative net force. Importantly, the large-magnitude atomic forces considerably increase from 300 K to 0.001 K, implying the local pinning enhancement induced by trapping in a deep state at low temperatures.

Next, we aim at relating the pinning sites with the Moiré superlattices to understand the role of a superlattice in friction. Fig. 5a depicts a schematic illustration of the potential energy landscape, which provides another viewpoint on the stick–slip motion. The stick stage can be considered as an elastic shear deformation between graphene and copper, in which the energy barrier connecting the initial and final local minima is reduced

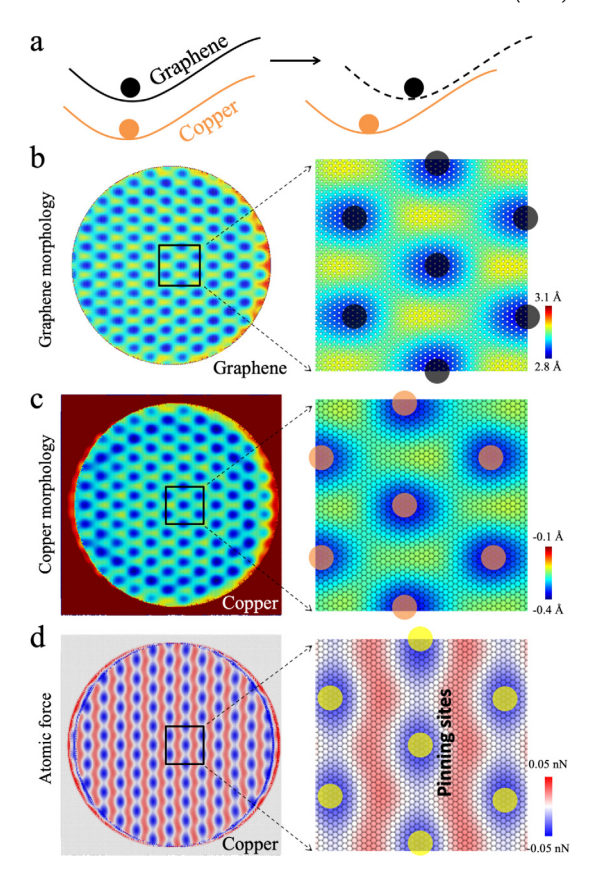


Fig. 5. Shearing (distortion) of artificial superlattices induces pinning sites and friction force against sliding. (a) Schematic illustration of landscape evolution in graphene sliding over copper. (b–c) The superlattice sites on graphene (b) and copper (d), which overlap in the initial state, are shifted along the lateral force direction during sliding. As shown in (d), the interfacial superlattice sites appear as enhanced pinning sites, resisting forward motion of graphene.

by the applied lateral force. When the system reaches a saddle point, and the corresponding energy barrier vanishes, the system relaxes into the new local energy minimum, resulting in a fast slip movement. In Fig. 5b-d, we present the graphene and copper morphologies, as well as the atomic forces at the critical saddle point. One can discern the superlattice sites on graphene and copper (Fig. 5b-c), which overlap each other in the initial state, are shifted along the motion direction due to the interfacial elastic shearing caused by the lateral force. In section three of the supplementary information, we discuss the superlattice translation caused by graphene slip motion in an arbitrary direction by deriving the mathematical relationship. As a result of this uniaxial force, the initial round-like superlattice site is twisted into an oval-like contour. These interfacial superlattices, being viewed as artificial lattice sites, are connected throughout attentive interaction. In response to the shear deformation, the superlattices on the copper surface drag the graphene and obstruct the shear motion (i.e., pinning sites shown in Fig. 5d). At a critical lateral force, the system overcomes the energy barrier, and slip motion takes place. The system, therefore, jumps to the adjacent one, corresponding to the slip motion, which causes the periodic shift of superlattice. These superlattices, enhancing the resistance of the interfacial motion, become weakened at high temperatures. This temperature-induced thermolubricity leads to a reduction of friction force, which is considered to the mechanisms responsible for the suppression of stick-slip friction in the copper-supported graphene system.

In conclusion, we revealed the atomic mechanisms behind thermally-induced friction behavior crossover from regular stickslip motion to a chaotic mode in two-dimensional materials. The distortion of stick-slip friction and reduction of friction force stem from temperature-dependent contact quality, characterizing interfacial fiction nature, and providing a complementary viewpoint to the true contact area. Specifically, we found the pinning sites originating from Moiré superlattice can transform into pushing spots due to nonconcurrent motion and promotes fiction motion, reducing friction resistance. Broadly, the results imply a way of tuning friction behavior via controlling or engineering interfacial superlattices.

Declaration of competing interest

The authors declare that they have no known competing financial interests or personal relationships that could have appeared to influence the work reported in this paper.

Acknowledgment

The authors acknowledge the support from School of Engineering at University of California, Irvine. P.C. acknowledges support from National Science Foundation under grant no. CMMI-1935371.

Appendix A. Supplementary data

Supplementary material related to this article can be found online at https://doi.org/10.1016/j.eml.2021.101273.

References

- D. Karnopp, Computer simulation of stick-slip friction in mechanical dynamic systems, J. Dyn. Syst. Meas. Control 107 (1985) 100.
- [2] M. Urbakh, J. Klafter, D. Gourdon, J. Israelachvili, The nonlinear nature of friction, Nature 430 (6999) (2004) 525–528.
- [3] L. Prandtl, Ein gedankenmodell zur kinetischen theorie der festen Körper, ZAMM-J. Appl. Math. Mech./ Z. Angew. Math. Mech. 8 (2) (1928) 85–106.
- [4] G. Tomlinson, Cvi. A molecular theory of friction, Lond. Edinb. Dublin Philos. Mag. J. Sci. 7 (46) (1929) 905–939.
- [5] M. Rozman, M. Urbakh, J. Klafter, Controlling chaotic frictional forces, Phys. Rev. E 57 (6) (1998) 7340.
- [6] A. Cochard, L. Bureau, T. Baumberger, Stabilization of frictional sliding by normal load modulation, J. Appl. Mech. 70 (2) (2003) 220–226.
- [7] X.-Z. Liu, Z. Ye, Y. Dong, P. Egberts, R.W. Carpick, A. Martini, Dynamics of atomic stick-slip friction examined with atomic force microscopy and atomistic simulations at overlapping speeds, Phys. Rev. Lett. 114 (14) (2015) 146102.
- [8] S.Y. Krylov, K. Jinesh, H. Valk, M. Dienwiebel, J. Frenken, Thermally induced suppression of friction at the atomic scale, Phys. Rev. E 71 (6) (2005) 065101.

- [9] L. Jansen, H. Hölscher, H. Fuchs, A. Schirmeisen, Temperature dependence of atomic-scale stick-slip friction, Phys. Rev. Lett. 104 (25) (2010) 256101.
- [10] X. Zhao, S.R. Phillpot, W.G. Sawyer, S.B. Sinnott, S.S. Perry, et al., Transition from thermal to athermal friction under cryogenic conditions, Phys. Rev. Lett. 102 (18) (2009) 186102.
- [11] M. Dienwiebel, G.S. Verhoeven, N. Pradeep, J.W. Frenken, J.A. Heimberg, H.W. Zandbergen, Superlubricity of graphite, Phys. Rev. Lett. 92 (12) (2004) 126101.
- [12] L. Gao, J.R. Guest, N.P. Guisinger, Epitaxial graphene on Cu (111), Nano Lett. 10 (9) (2010) 3512–3516.
- [13] R. He, L. Zhao, N. Petrone, K.S. Kim, M. Roth, J. Hone, P. Kim, A. Pasupathy, A. Pinczuk, Large physisorption strain in chemical vapor deposition of graphene on copper substrates, Nano Lett. 12 (5) (2012) 2408–2413.
- [14] P. Egberts, G.H. Han, X.Z. Liu, A.C. Johnson, R.W. Carpick, Frictional behavior of atomically thin sheets: hexagonal-shaped graphene islands grown on copper by chemical vapor deposition, ACS Nano 8 (5) (2014) 5010–5021.
- [15] Y. Mishin, M. Mehl, D. Papaconstantopoulos, A. Voter, J. Kress, Structural stability and lattice defects in copper: Ab initio, tight-binding, and embedded-atom calculations, Phys. Rev. B 63 (22) (2001) 224106.
- [16] S.J. Stuart, A.B. Tutein, J.A. Harrison, A reactive potential for hydrocarbons with intermolecular interactions, J. Chem. Phys. 112 (14) (2000) 6472–6486.
- [17] M. Fuentes-Cabrera, B.H. Rhodes, J.D. Fowlkes, A. López-Benzanilla, H. Terrones, M.L. Simpson, P.D. Rack, Molecular dynamics study of the dewetting of copper on graphite and graphene: Implications for nanoscale self-assembly, Phys. Rev. E 83 (4) (2011) 041603.
- [18] S. Nosé, A molecular dynamics method for simulations in the canonical ensemble, Mol. Phys. 52 (2) (1984) 255–268.
- [19] W.G. Hoover, Canonical dynamics: Equilibrium phase-space distributions, Phys. Rev. A 31 (3) (1985) 1695.
- [20] D. Mandelli, W. Ouyang, O. Hod, M. Urbakh, Negative friction coefficients in superlubric graphite-hexagonal boron nitride heterojunctions, Phys. Rev. Lett. 122 (7) (2019) 076102.
- [21] S. Li, Q. Li, R.W. Carpick, P. Gumbsch, X.Z. Liu, X. Ding, J. Sun, J. Li, The evolving quality of frictional contact with graphene, Nature 539 (7630) (2016) 541–545.
- [22] J.H. Kang, J. Moon, D.J. Kim, Y. Kim, I. Jo, C. Jeon, J. Lee, B.H. Hong, Strain relaxation of graphene layers by Cu surface roughening, Nano Lett. 16 (10) (2016) 5993–5998.
- [23] D.G. Truhlar, B.C. Garrett, S.J. Klippenstein, Current status of transition-state theory, J. Phys. Chem. 100 (31) (1996) 12771–12800.
- [24] Y. Fan, P. Cao, Long time-scale atomistic modeling and simulation of deformation and flow in solids, Handb. Mater. Model.: Appl.: Curr. Emerg. Mater. (2020) 237–263.
- [25] Y. Fan, Y.N. Osetskiy, S. Yip, B. Yildiz, Mapping strain rate dependence of dislocation-defect interactions by atomistic simulations, Proc. Natl. Acad. Sci. 110 (44) (2013) 17756–17761.
- [26] Y. Fan, Y.N. Osetsky, S. Yip, B. Yildiz, Onset mechanism of strain-rate-induced flow stress upturn, Phys. Rev. Lett. 109 (13) (2012)
- [27] P. Cao, M.P. Short, S. Yip, Potential energy landscape activations governing plastic flows in glass rheology, Proc. Natl. Acad. Sci. 116 (38) (2019) 18790–18797.
- [28] Y. Mo, K.T. Turner, I. Szlufarska, Friction laws at the nanoscale, Nature 457 (7233) (2009) 1116–1119.